



Research Article

The First-Principles Study On The Investigation of Magnetic and Electronic Properties of Ga₄X₃Mn (X = P and As)

Aytaç ERKİŞİ*¹

¹*Pamukkale University, Department of Physics, 20070, Denizli, Turkey*

**corresponding author e-mail: aerkisi@pau.edu.tr*

(Alınış / Received: 07.06.2022, Kabul / Accepted: 21.09.2022, Yayınlanma / Published: 25.11.2022)

Abstract: In this study, the magnetic nature and also, electronic characteristics of Ga₄X₃Mn (X=P and As) systems, which have simple cubic structure confirming $P\bar{4}3m$ space group and 215 space number, have been reported. All calculations realized within the framework of *ab initio* simulation methods have been performed using the meta-generalized gradient (META-GGA) approach within the Density Functional Theory (DFT). In view of the energy-volume curves and the calculated cohesive and formation energies for considering four different types of magnetic orders, it has been detected that these compounds have A-type antiferromagnetic nature. Also, the examined electronic behaviors in the A-type antiferromagnetic order of the related systems show that all two compounds are semiconductors due to having small band gaps in their electronic band structures ($E_g = 0.23$ eV for Ga₄P₃Mn and $E_g = 0.16$ eV for Ga₄As₃Mn).

Key words: Semiconductor, Antiferromagnetism, *Ab initio* calculations, Density functional theory.

Ga₄X₃Mn (X = P and As)'in Manyetik ve Elektronik Özelliklerinin İncelenmesi Üzerine İlk İlkeler Çalışması

Öz: Bu çalışmada, basit kübik yapıya sahip ve $P\bar{4}3m$ uzay grubu ile 215 uzay numarasına uyan Ga₄X₃Mn (X=P and As) sistemlerinin manyetik doğası ve ayrıca elektronik karakteristiği rapor edilmiştir. *Ab initio* simülasyon yöntemleri çerçevesinde gerçekleştirilen tüm hesaplamalar, Yoğunluk Fonksiyonel Teorisi (YFT) kapsamında meta-genelleştirilmiş gradient (META-GGA) yaklaşımı kullanılarak yapılmıştır. Dört farklı tip manyetik düzen için enerji-hacim eğrileri ve hesaplanan kohesif ve oluşum enerjileri göz önüne alındığında, bu bileşiklerin A-tipi antiferromanyetik yapıya sahip oldukları tespit edilmiştir. Ayrıca ilgili sistemlerin A-tipi antiferromanyetik düzende incelenen elektronik davranışları, elektronik bant yapılarında küçük bant boşluklarına sahip olmaları nedeniyle yarı-iletken olduklarını göstermektedir (Ga₄P₃Mn için $E_b = 0.23$ eV ve Ga₄As₃Mn için $E_b = 0.16$ eV).

Anahtar kelimeler: Yarı-iletken, Antiferromanyetizma, *ab initio* hesaplamaları, Yoğunluk fonksiyonel teorisi.

1. Introduction

In recent years, interest in materials exhibiting remarkable electronic and optical properties such as GaAs and GaP has increased considerably. In particular, their usefulness for photovoltaic and quantum dot solar-cell applications has made such materials the focus of attention [1-5]. Among them, a research group studied the electronic characteristic of these types of compounds by using the exact exchange method computationally [6]. In particular, some experimental studies on the photoluminescence and electrical properties of InAs and GaAs compounds, which will help to understand why they are so effective in solar cell applications, have been attracted [7-10]. Apart from these, there are many studies in the literature regarding the magnetic susceptibility and optoelectronic properties of such compounds [11-13].

Also, in some of the theoretical studies, the electronic behavior of GaAsX and GaPX type compounds, where X was chosen from a transition metal, was reported [14-16]. In one of the previous studies, The observed ferromagnetic-type splitting of fundamental absorption edge in ferromagnetic $\text{Ga}_{1-x}\text{Mn}_x\text{As}$ ($x < 0.05$) epilayers was explained by antiferromagnetic $p - d$ exchange interaction [17]. In another theoretical study, the magnetic nature of (Ga, Mn)As systems was examined by using the pseudopotential self-interaction correction (pSIC) and maximally-localized Wannier functions (MLWFs) [18]. Especially, in the reference study, in which the phonon dispersion of GaAs, GaP, $\text{Ga}_3\text{As}_4\text{Ti}$, and $\text{Ga}_3\text{P}_4\text{Ti}$ compounds was presented, the vibrational properties of these compounds have led me to focus on the magnetic and electronic nature of $\text{Ga}_4\text{X}_3\text{Mn}$ (X=P and As) compounds [19]. Furthermore, the fact that in an *ab initio* study on the electronic nature of $\text{Ti}_x\text{Ga}_{1-x}\text{P}$ ($x = 0.3125 - 0.25$) reported that these compounds have a half-metallic nature [20-22], which is extremely important from a technological point of view, has increased the motivation in this study.

In this computational study, the antiferromagnetic nature with semiconducting behavior of $\text{Ga}_4\text{X}_3\text{Mn}$ (X=P and As) compounds has been presented by using *ab initio* simulation methods under strongly constrained and appropriately normed semi-local density functional, meta-generalized gradient (METAGGA-SCAN) approximation. It has been determined that the most stable magnetic order for the mentioned compounds is A-type antiferromagnetic and by examining the electronic band structures in this magnetic phase, it has been detected that they have a semiconductor nature. These novel compositions have been focused on since such gallium-based cubic structures exhibit good physical properties that can be useful in technological applications such as semiconductor behavior. In this context, the aim of this computational study based on density functional theory, is to add new systems to wide semiconductor family. The computed results show that the related systems have A-type antiferromagnetic nature with semiconducting behavior. So, the mentioned compounds could have in opto-electronic applications.

2. Material and Method

In this presented study, the necessary computations to investigate the magnetic nature and electronic behavior of the related compounds, have been performed under density functional theory (DFT) utilizing VASP (Vienna Ab initio Simulation Package) [23-25] software. Also, the projector augmented wave (PAW) [26-28] method has been employed to describe electron-ion interactions. Furthermore, for the electron-electron interactions between the atoms in the related systems, Perdew–Burke–Ernzerhof (PBE) [29] type pseudopotentials under METAGGA-SCAN [30] approach have been used. For *Ga*, *P*, *As*

and *Mn* atoms in the mentioned compositions, the valence electron configurations are as follows: $3d^{10}4s^24p^1$, $3s^23p^3$, $3d^{10}4s^24p^3$ and $3d^64s^1$.

During the optimization process to obtain the best structural parameters of the primitive cells of these systems, the reciprocal space has been modeled with an automatically generated $12 \times 12 \times 12$ Monkhorst-Pack [31] scheme giving 56 k-points. For the plane waves in expansion, the kinetic energy cut-off value has been fixed at 900 eV. To relax the ions in primitive cells of the mentioned systems, the quasi-Newton method has been utilized until the forces on the atoms are small than 10^{-8} eV/Å. Also, the energy convergence criterion in successive iteration steps in which Kohn-Sham equations are solved, has been chosen as 10^{-9} eV. For the primitive cells of these cubic systems, the optimization processes in which are obtained best suitable structural parameters, have been carried out until minimizing the forces and the pressures on the related compositions. Then, for each system, a $2 \times 2 \times 2$ supercell consisting of 64 atoms has been created and energy-volume values in the considered four different types of magnetic order, have been calculated to detect the most stable magnetic phase.

3. Results

In the presented computational study, initially, the primitive cells of cubic $\text{Ga}_4\text{X}_3\text{Mn}$ ($\text{X}=\text{P}$ and As) systems have been appropriately optimized to locate the ions at the most favorable Wyckoff [32] positions of the cell and obtain structural parameters with great accuracy. The primitive cell of each mentioned composition, which is illustrated in below Figure 1, consists of 8 atoms and crystallizes in a simple cubic structure with the $P\bar{4}3m$ space group and 215 space number. As shown in this Figure, in the well optimized cells, four gallium (*Ga*) atoms are located at 4e ((0.257, 0.257, 0.257) for $\text{Ga}_4\text{P}_3\text{Mn}$, (0.253, 0.253, 0.253) for $\text{Ga}_4\text{As}_3\text{Mn}$) while one manganese (*Mn*) atom and three phosphorus (*P*) (or arsenic (*As*)) atoms are placed on 1a (0, 0, 0) and 3c (0.5, 0.5, 0), respectively. Furthermore, for each system, to detect the most stable magnetic order by using energy-volume graphs, supercells containing 64 atoms, have been created.

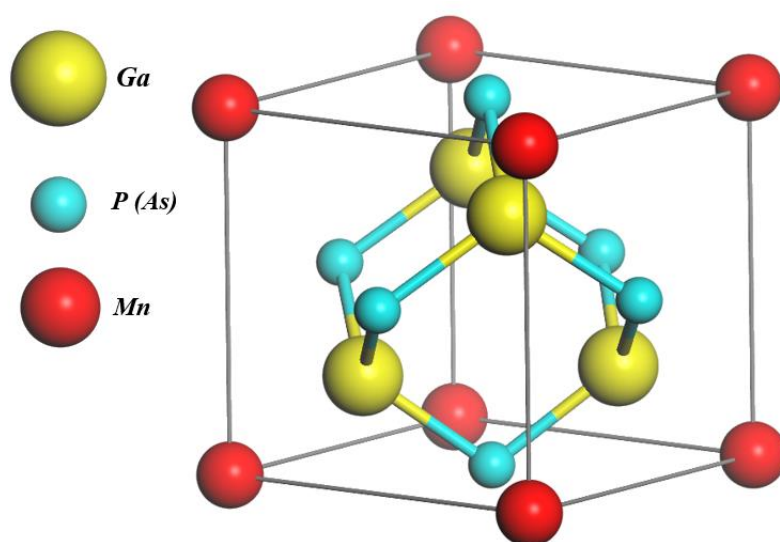


Figure 1. The three-dimensional crystallization of the primitive cells of cubic $\text{Ga}_4\text{X}_3\text{Mn}$ ($\text{X}=\text{P}$ and As) systems.

3.1. The detected most suitable magnetic arrangement

There is a close relationship between the antiferromagnetism nature of solid crystals and the orientation of magnetic moments of atoms. Usually, a typical antiferromagnetic system behaves like two ferromagnetic subsystems in which the spins of neighbor atoms are in opposite directions and though the total magnetic moment of each subsystem is different from zero, the total magnetic moment of the whole antiferromagnetic system is equal to zero. So, a material having this type of magnetic nature does not generate magnetization. It is known that there are three different types of antiferromagnetic order according to the arrangement of the magnetic moments of the atoms. These are A-type, C-type, and G-type [33] which have been schematically represented in Figure 2.

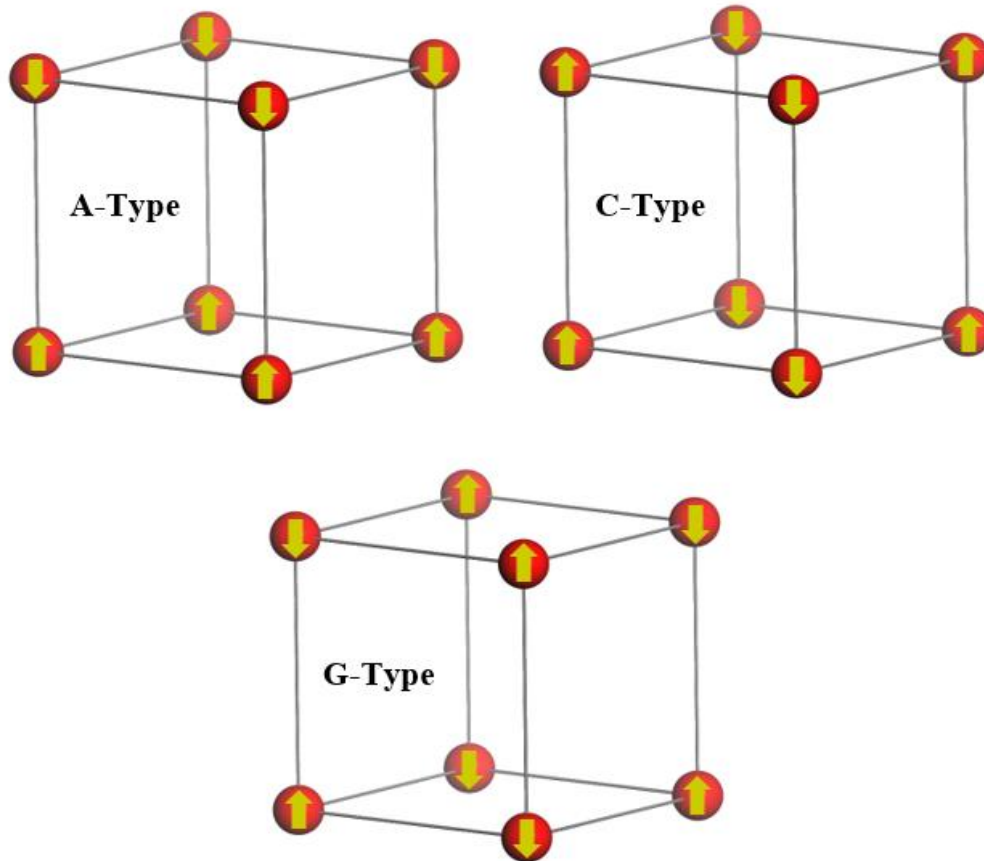


Figure 2. For three different types of antiferromagnetic arrangements, the orientation of magnetic moments of manganese (Mn) atoms in the related compositions having a simple cubic structure.

In order to determine the most favorable magnetic order of the related systems, four different types of arrangements have been considered A-type antiferromagnetic (A-AFM), C-type antiferromagnetic (C-AFM), G-type antiferromagnetic (G-AFM) and ferromagnetic (FM). In antiferromagnetic arrangements, the magnetic moments of the manganese (Mn) atoms have been aligned antiparallel, resulting in zero total magnetizations for all systems in this study. For the ferromagnetic arrangement, the magnetic moments of the atoms have been ordered in the same direction. Also, for these systems, the cohesive and formation energies have been calculated in each of four different magnetic orders. The cohesive energy is required to dissociate a crystal into free constituent atoms and can be calculated from the ground state energy difference between

the isolated free atoms and bulk crystal [34]. The formation energy is generally used to obtain information about the thermodynamic stability and the structural synthesizability of any crystal system. The related energy value can be calculated from the internal energy variations [35]. It is well known that the negative formation energy indicates the thermodynamical stability and the structural synthesizability of the interesting material. Also, when the calculated formation or cohesive energy for any structural or magnetic phase, is smaller than the other phases, it can be said that, in energetically, this phase is more favorable for the compound. In this regard, it can be understood that the more favorable magnetic arrangement for $\text{Ga}_4\text{X}_3\text{Mn}$ ($\text{X}=\text{P}$ and As) compounds is A-AFM, as seen in Table 1. Moreover, these compositions are stable thermodynamically due to the calculated negative formation energy values. So, under ambient conditions, they can be synthesized to be used in possible applications in technology. Then, the energy-volume curves obtained by fitting energy and volume data to the Vinet equation of states [36], have been plotted for each magnetic order, as shown in Figure 3. It can be clearly observed from these graphs that the more favorable magnetic phase energetically for the related systems is A-AFM and this is exactly consistent with the calculated cohesive and formation energy values as seen in Table 1.

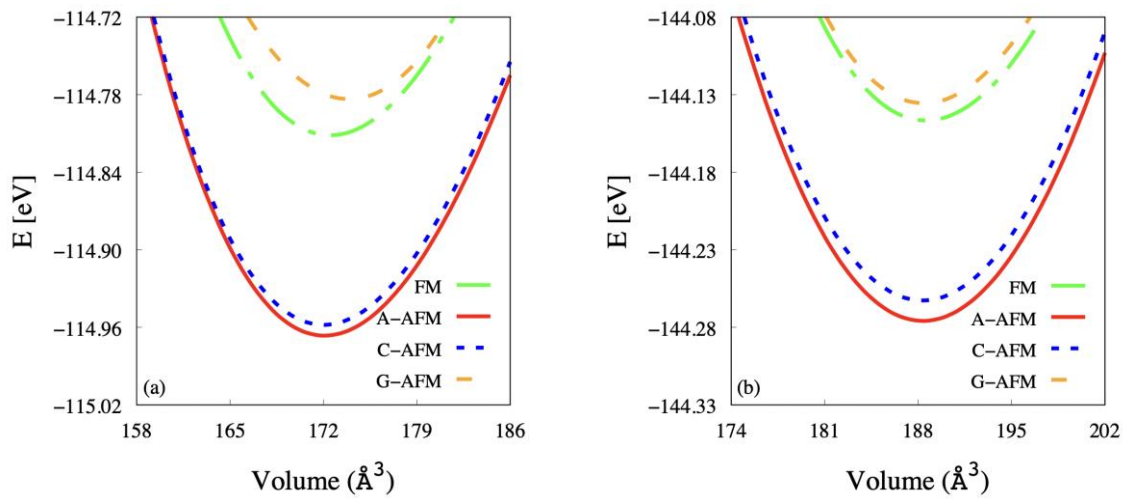


Figure 3. The total energies of the primitive cell as a function of volume in FM, A-AFM, C-AFM, and G-AFM orders within METAGGA-SCAN of the cubic (a) $\text{Ga}_4\text{P}_3\text{Mn}$ and (b) $\text{Ga}_4\text{As}_3\text{Mn}$ compositions.

Table 1. The optimized lattice parameters (a in \AA), the cohesive (E_{coh} in eV) and formation energy values (E_{for} in eV) of cubic $\text{Ga}_4\text{X}_3\text{Mn}$ ($\text{X}=\text{P}$ and As) systems for different types of magnetic orders.

Material	Magnetic Order	a [\AA]	E_{coh} [eV]	E_{for} [eV]
$\text{Ga}_4\text{P}_3\text{Mn}$	FM	5.566	- 26.301	- 0.164
	A-AFM	5.561	- 26.456	- 0.319
	C-AFM	5.561	- 26.448	- 0.311
	G-AFM	5.567	- 26.270	- 0.133
$\text{Ga}_4\text{As}_3\text{Mn}$	FM	5.734	- 25.445	- 0.085
	A-AFM	5.727	- 25.574	- 0.214
	C-AFM	5.727	- 25.561	- 0.201
	G-AFM	5.732	- 25.433	- 0.073

As given in Table 1 and Figure 3, phosphorus (*P*) atoms increase stability in energetically while arsenic (*As*) atoms decrease, since the energy values of the $\text{Ga}_4\text{P}_3\text{Mn}$ system are lower than the other system. To the best of my knowledge from the literature, there is no available study in experimentally or theoretically about the related compounds to make any comparison with the obtained results in this study. Furthermore, the measured bond lengths in the primitive cell by using the VESTA program [37] between *Ga* and *P* atoms and between *Mn* and *P* atoms for $\text{Ga}_4\text{P}_3\text{Mn}$ compound are 2.39 Å and 3.94 Å, respectively, whereas between *Ga* and *As* atoms and between *Mn* and *As* atoms for $\text{Ga}_4\text{As}_3\text{Mn}$ compound are 2.47 Å and 4.05 Å, respectively. In theoretically, it is well known that the shorter bond lengths in the primitive cell of any crystal mean higher bond energy and therefore, a short atomic bond is less likely to break. In this aspect, it can be concluded that energetic stability increases in such compositions containing phosphorus than containing arsenic atoms.

3.2. The electronic behavior in a-type antiferromagnetic order

After it was detected that these ternary cubic systems have A-type antiferromagnetic behavior in their ground states, their electronic band structures were observed under the METAGGA-SCAN method. Along the high-symmetry directions in the Brillouin zone, the energy band structures and the total density of electronic states (TDOS) of these systems having an A-AFM magnetic nature, were plotted, as seen in Figure 4 and Figure 5. As clearly understood from the plotted Figures these ternary cubic compounds can be classified as semiconductor materials since there are small band gaps ($E_g = 0.23$ eV for $\text{Ga}_4\text{P}_3\text{Mn}$ and $E_g = 0.16$ eV for $\text{Ga}_4\text{As}_3\text{Mn}$) in their observed electronic band structures. Also, the great similarity between spin-up and spin-down states indicates the antiferromagnetic nature of the mentioned systems in this study. This observed situation is consistent with the previous section where the magnetic behavior of the systems concerned was determined. For both two systems, the obtained band gaps are indirect from R to Γ point.

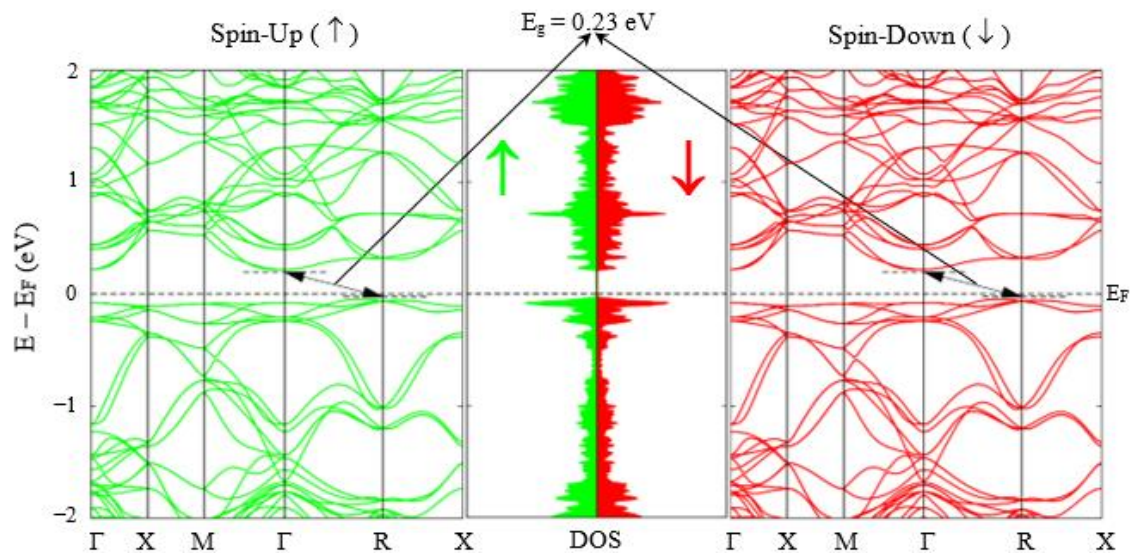


Figure 4. The observed energy band structure with the total density of electronic states within METAGGA-SCAN of $\text{Ga}_4\text{P}_3\text{Mn}$ system.

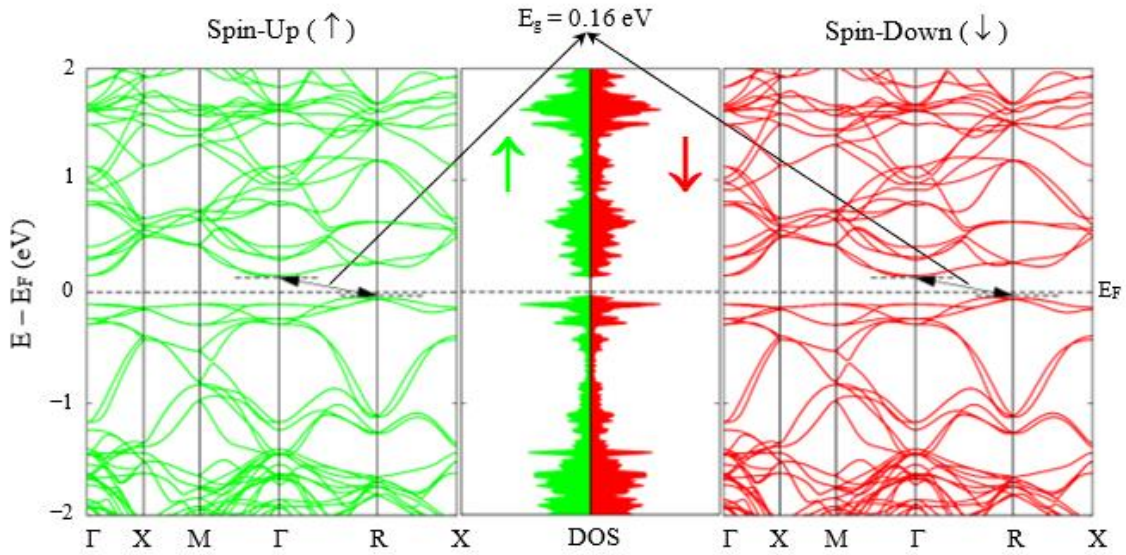


Figure 5. The observed energy band structure with the total density of electronic states within METAGGA-SCAN of $\text{Ga}_4\text{As}_3\text{Mn}$ system.

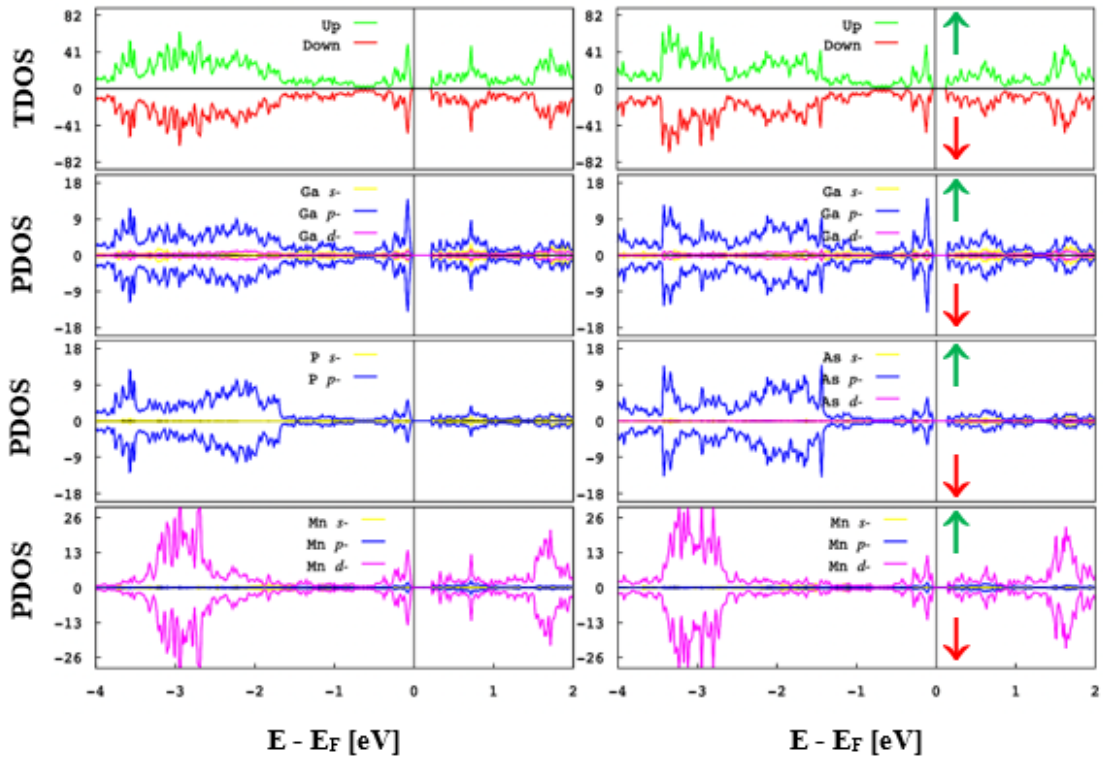


Figure 6. The TDOS and orbital projected PDOS of atoms within METAGGA-SCAN of (a) $\text{Ga}_4\text{P}_3\text{Mn}$ and (b) $\text{Ga}_4\text{As}_3\text{Mn}$ systems.

Furthermore, to understand better which orbitals of atoms play a dominant role in the semi-conducting nature of these systems, the partial density of electronic states of atoms (PDOS) was plotted, as seen in below Figure 6 (a) and Figure 6 (b). In the presented Figures, the d -orbitals of manganese (Mn) atoms and the p -orbitals of gallium (Ga) atoms are dominant in the conduction band which is above Fermi level (E_F), in a wide energy range. In the valence band which is below Fermi level (E_F), around E_F , for both systems,

there are hybridizations between $3d$ states of Mn atoms and p -orbitals of Ga and P (As) atoms. In the same band, the hybridizations can be observed between $4p$ states of Ga atoms and $3p$ states of P atoms (almost between -1.7 eV and -2 eV) for the Ga_4P_3Mn system. Also, for the Ga_4As_3Mn system, there are remarkable hybridizations between $4p$ states of Ga and As atoms (almost between -1.4 eV and -2 eV) too. In this view, it can be clearly concluded from the related Figures that the semiconducting characteristic of these systems is mainly attributed to the p orbitals of the Ga and P (As) atoms and also, the d orbitals of the Mn atoms. The s orbitals of atoms, d orbitals of the Ga atoms, and also, p orbitals of the Mn atoms in these systems don't affect so much their electronic nature.

Also, to obtain information about atomic bonding type in the primitive cell of these systems, two-dimensional charge-density distributions were plotted for (100) and (110) planes as given in Figure 7. The mentioned graphs indicate that transition metal atoms Mn make ionic bonds while P and As atoms which are usually named p -block elements in the periodic table, and Ga atoms make covalent bonds with each other. In this subsection, only the distribution of the Ga_4As_3Mn system is presented, since the distributions plotted for Ga_4P_3Mn are very similar to the distributions plotted for Ga_4As_3Mn .

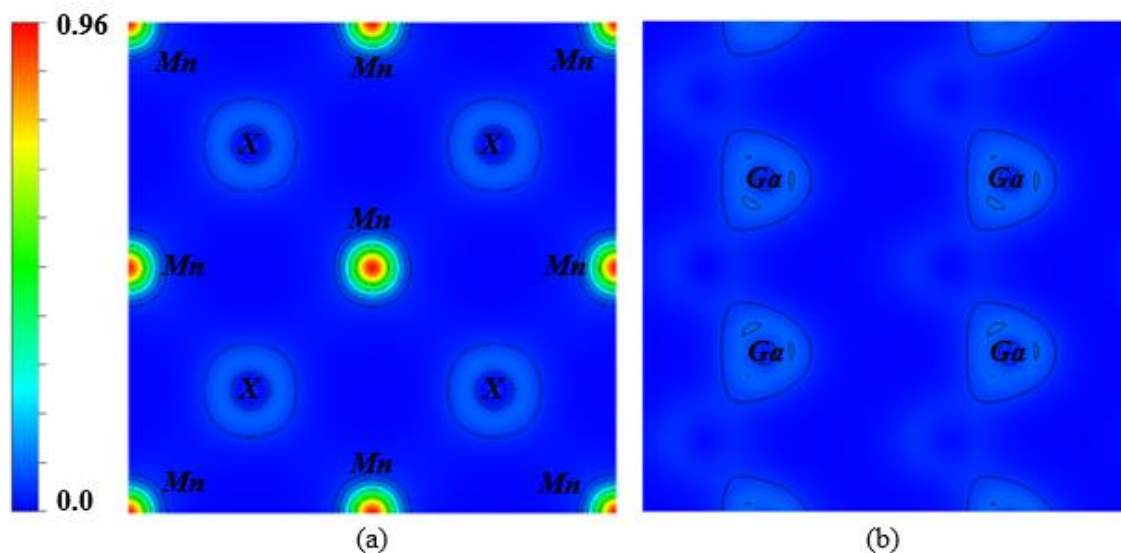


Figure 7. The charge distribution (in units of e) of cubic Ga_4X_3Mn ($X=P$ and As) systems for (a) (100) plane and (b) (110) plane.

Additionally, to obtain information about the charge of each ion in these systems, the analysis of the Bader partial charge was carried out. The analyzed Bader net partial charges were listed in Table 2 and in the related Table, the total Bader net charge is equal to zero for both of the two compositions. The negative value of the Bader charge indicates that the charge is transferred to the atom, while the positive value means that the charge moves away from the atom [38]. Accordingly, for the Ga_4P_3Mn system, the Mn and Ga atoms give electrons to the P atoms, whereas, for the Ga_4As_3Mn system, the Mn and As atoms give electrons to the Ga atoms.

Table 2. Bader partial net charges (in units of e) for *Ga*, *P* (*As*) and *Mn* atoms in ternary cubic Ga_4X_3Mn ($X=P$ and As) systems.

Material	<i>Ga</i>	<i>P</i>	<i>As</i>	<i>Mn</i>
Ga_4P_3Mn	2.0398	-3.9296	-	1.8898
Ga_4As_3Mn	-1.8878	-	1.0755	0.8123

4. Conclusion

In this study, it was carried out comprehensive *ab initio* calculations under METAGGA-SCAN approximation to reveal the magnetic and electronic characteristic of ternary cubic Ga_4X_3Mn ($X=P$ and As) systems which are crystallized in simple cubic structure conforming $P\bar{4}3m$ space group and 215 space number. For the related compositions, the drawn energy-volume graphs, and also the calculated cohesive and formation energy values show that the most suitable magnetic phase energetically among the considered four different types of magnetic orders is A-type antiferromagnetic. Moreover, the negative formation energy values indicate the thermodynamical stability and the structural synthesizability of the materials. Also, it can be understood from the atomic bond lengths that the energetic stability increases in such compositions containing phosphorus than containing arsenic atoms. The observed electronic band structures in the A-AFM order indicate the semiconducting character of these materials due to having the indirect band gaps ($E_g = 0.23$ eV for Ga_4P_3Mn and $E_g = 0.16$ eV for Ga_4As_3Mn) in both spin-states. Furthermore, the performed Bader charge analyzes show that while *Mn* and *Ga* atoms donate electrons to *P* atoms in the Ga_4P_3Mn system, *Mn* and *As* atoms donate electrons to *Ga* atoms in the Ga_4As_3Mn system. In this regard, the mentioned materials in this study could be good candidates for especially semiconductor devices.

Author Statement

Aytaç Erkişi: Investigation, Validation, Review and Editing, Original Draft Writing.

Acknowledgment

This research was supported in part by TÜBİTAK (The Scientific & Technological Research Council of Turkey) through TR-Grid e-Infrastructure Project, part of the calculations has been carried out at ULAKBİM Computer Center.

Conflict of Interest

As the author of this study, I declare that I do not have any conflict of interest statement.

Ethics Committee Approval and Informed Consent

As the author of this study, I declare that I do not have any ethics committee approval and/or informed consent statement.

References

- [1] S. Mahajan, *Handbook of Semiconductors*, Elsevier, Amsterdam, 1994.
- [2] X. Yang, K. Wang, Y. Gu, H. Ni, X. Wang, T. Yang, and Z. Wang, "Improved efficiency of InAs/GaAs quantum dots solar cells by Si-doping," *Sol. Energ. Mat. Sol. C.*, 113, 144-147, 2013.

- [3] P.G. Linares, A. Marti, E. Antolin, I. Ramiro, E. Lopez, E. Hernandez, D.F. Marron, I. Artacho, I. Tobias, P. Gerard, C. Chaix, R.P. Campion, C.T. Foxon, C.R. Stanley, S.I. Molina, and A. Luque, "Extreme voltage recovery in GaAs:Ti intermediate band solar cells," *Sol. Energ. Mat. Sol. C.*, 108, 175-179, 2013.
- [4] A. Luque and A. Marti, "The intermediate band solar cell: progress toward the realization of an attractive concept," *Adv. Mater.*, 22, 160-174, 2010.
- [5] P. Lama, S. Hacha, J. Wua, M. Tanga, V. G. Dorogan, Y. I. Mazur, G. J. Salamo, I. Ramiro, A. Seeds, and H. Liu, "Voltage recovery in charged InAs/GaAs quantum dot solar cells," *Nano Energy*, 6, 159-166, 2014.
- [6] J.J. Fernandez, C. Tablero, and P. Wahnnon, "Development and implementation of the exact exchange method for semiconductors using a localized basis set," *Comput. Mater. Sci.*, 28, 274-286, 2003.
- [7] T. Kita, R. Hasagawa, and T. Inoue, "Suppression of nonradiative recombination process in directly Si-doped InAs/GaAs quantum dots," *J. Appl. Phys.*, 110, 103511, 2011.
- [8] W. Liu, X. D. Wang, Y. Q. Li, Z. X. Geng, F. H. Yang, and J. M. Li, "Surface plasmon enhanced GaAs thin film solar cells," *Sol. Energy Mater. Sol. Cells*, 95, 693-698, 2011.
- [9] K.F. Wang, Y.X. Gu, X.G. Yang, T. Yang, and Z. G. Wang, "Si delta doping inside InAs/GaAs quantum dots with different doping densities," *J. Vac. Sci. Technol. B*, 30, 041808, 2012.
- [10] K.A. Sablon, J.W. Little, V. Mitin, A. Sergeev, N. Vagidov, and K. Reinhardt, "Strong enhancement of solar cell efficiency due to quantum dots with built-in charge," *Nano Letters*, 11, 2311-2317, 2011.
- [11] M.K. Elsaid and E. Hijaz, "Magnetic susceptibility of coupled double GaAs quantum dot in magnetic fields," *Acta Phys. Pol. A*, 131, 1491-1496, 2017.
- [12] M. Perny, V. Saly, V. Durman, J. Packa, J. Kurcz, M. Mikolasek, and J. Huran, "Electrical response of silicon heterojunction solar cells with transparent conductive oxide antireflective coating," *Acta Phys. Pol. A*, 139, 39-45, 2021.
- [13] B. Pustelny and T. Pustelny, "Transverse acoustoelectric effect applying in surface study of GaP:Te(111)," *Acta Phys. Pol. A*, 116, 383-384, 2009.
- [14] P. Wahnnon and C. Tablero, "Ab initio electronic structure calculations for metallic intermediate band formation in photovoltaic materials," *Phys. Rev. B*, 65, 165115, 2002.
- [15] T. Ponken and T. Burinprakhon, "Microstructure, optical and electrical properties of thin films of galliumphosphorus - titanium alloys synthesized by asymmetric bipolar pulsed direct current magnetron sputtering," *Thin Solid Films*, 681, 6-14, 2019.
- [16] C. Tablero, P. Wahnnon, "Analysis of metallic intermediate-band formation in photovoltaic materials," *Appl. Phys. Lett.*, 82, 151-153, 2003.
- [17] J. Szczytko, W. Mac, A. Twardowski, F. Matsukura, and H. Ohno, "Antiferromagnetic $p-d$ exchange in ferromagnetic $\text{Ga}_{1-x}\text{Mn}_x\text{As}$ epilayers," *Phys. Rev. B*, 59, 12935, 1999.
- [18] K. Z. Milowska and M. Wierzbowska, "Hole sp^3 - character and delocalization in (Ga, Mn)As revised with pSIC and MLWF approaches - Newly found spin-unpolarized gap states of s -type below 1% of Mn," *Chem. Phys.*, 430, 7-12, 2014.
- [19] P. Palacios, P. Wahnnon, and C. Tablero, "Ab initio phonon dispersion calculations for $\text{Ti}_x\text{Ga}_n\text{As}_m$ and $\text{Ti}_x\text{Ga}_n\text{P}_m$ compounds," *Comput. Mater. Sci.*, 33, 118-124, 2005.
- [20] P. Palacios, J. J. Fernandez, K. Sanchez, J. C. Conesa, and P. Wahnnon, "First-principles investigation of isolated band formation in half-metallic $\text{Ti}_x\text{Ga}_{1-x}\text{P}$ ($x = 0.3125-0.25$)," *Phys. Rev. B*, 73, 085206, 2006.
- [21] J.J. Fernandez, C. Tablero, and P. Wahnnon, "Application of the exact exchange potential method for half metallic intermediate band alloy semiconductor," *J. Chem. Phys.*, 120, 10780-10785, 2004.
- [22] C. Tablero, A. Garcia, J. J. Fernandez, P. Palacios, and P. Wahnnon, "First principles characterization of direct transitions for high efficiency new photovoltaic materials," *Comput. Mater. Sci.*, 27, 58-64, 2003.
- [23] P. E. Blöchl, "Projector augmented-wave method," *Phys. Rev. B*, 50, 17953-17979, 1994.
- [24] W. Kohn and L. J. Sham, "Self-Consistent equations including exchange and correlation effects," *Phys. Rev. A*, 140, A1133-A1138, 1965.
- [25] P. Hohenberg and W. Kohn, "Inhomogeneous Electron Gas," *Phys. Rev.*, 136, B864-B871, 1964.
- [26] G. Kresse and J. Hafner, "Ab initio molecular dynamics for liquid metals," *Phys. Rev. B*, 47, 558-561, 1993.
- [27] G. Kresse and J. Furthmüller, "Efficient iterative schemes for ab initio total-energy calculations using a plane-wave basis set," *Phys. Rev. B*, 54, 11169, 1996.
- [28] G. Kresse and D. Joubert, "From Ultrasoft Pseudopotentials to the Projector Augmented-Wave Method," *Phys. Rev. B*, 59, 1758, 1999.
- [29] J. P. Perdew, K. Burke, and M. Ernzerhof, "Generalized gradient approximation made simple," *Phys. Rev. Lett*, 77, 3865-3868, 1996.

- [30] J. Sun, A. Ruzsinszky, and J. P. Perdew, "Strongly Constrained and Appropriately Normed Semilocal Density Functional," *Phys. Rev. Lett.*, 115, 036402, 2015.
- [31] H. J. Monkhorst and J. D. Pack, "Special points for Brillouin-zone integrations," *Phys. Rev. B*, 13, 5188-5192, 1976.
- [32] R. W. G. Wyckoff, *Crystal Structures*, Wiley, New York, 1963.
- [33] F. Han, *A Modern Course in the Quantum Theory of Solids*, World Scientific, Singapore, 2013.
- [34] A. L. Parrill and K. B. Lipkowitz, *Reviews in Computational Chemistry*, 29, 44-47, Wiley, 2016.
- [35] E. Zhao and Z. Wu, "Electronic and mechanical properties of 5d transition metal mononitrides via first principles," *J. Solid State Chem.*, 181, 2814-2827, 2008.
- [36] P. Vinet, J. H. Rose, J. Ferrante, and J. R. Smith, "Universal features of the equation of state of solids," *J. Phys. Cond. Matter*, 1, 1941-1963, 1989.
- [37] K. Momma and F. Izumi, "VESTA: a three-dimensional visualization system for electronic and structural analysis," *Appl. Crystallogr.*, 41, 653-658, 2008.
- [38] A. Gencer and G. Surucu, "Electronic and lattice dynamical properties of Ti₂SiB MAX phase" *Mater. Res. Express*, 5, 076303, 2018.